Supporting Information

Deeper insight into the Mechanisms behind Sputter Damage in Silicon Solar Cells based on the Example of Nanocrystalline Silicon Carbide

Alexander Eberst, Binbin Xu, Karsten Bittkau, Weiyuan Duan, Andreas Lambertz, Ansgar Meise, Marc Heggen, Rafal E. Dunin-Borkowski, Uwe Rau, Kaining Ding*

Table S1 shows the electrical conductivity of the nanocrystalline hydrogenated silicon carbide (nc-SiC:H) layers before the sputtering process, as well as after the ITO deposition with the ITO etched off and after an additional annealing step at 230°C for 20 min in ambient air and for the reverse processing order. Within the error of the measurement setup, the electrical conductivities stay approximately constant.

Table S1. Electrical conductivity before ITO deposition, after ITO deposition with the ITO etched off and after an additional annealing step at 230°C for 20 min in ambient air. Within the error of the measurement setup, the conductivity is approximately constant.

Step	Electrical conductivity σ [S/cm]
Initial	$1.1x10^{-1}±1x10^{-1}$
ITO → etch (no anneal)	$3.4x10^{-1}±1x10^{-1}$
ITO → anneal → etch	$9.9x10^{-1}±1x10^{-1}$
ITO → etch → anneal	$2.6 x10^{-1}±1x10^{-1}$

S1. Additional Simulations for Electron Penetration

Figure S1 shows the simulated penetration depth of electrons for a) a varying crystallinity of the nc-SiC:H(n) layer and b) a varying hydrogen content of the nc-SiC:H layer. Only a negligible decrease of 0.4 nm in maximum penetration depth with an increase in hydrogen content from 0 at% to 20 at% is visible. The deepest penetration is 4 nm at a hydrogen content of 0 at%. A lower crystallinity leads to a deeper penetration depth.

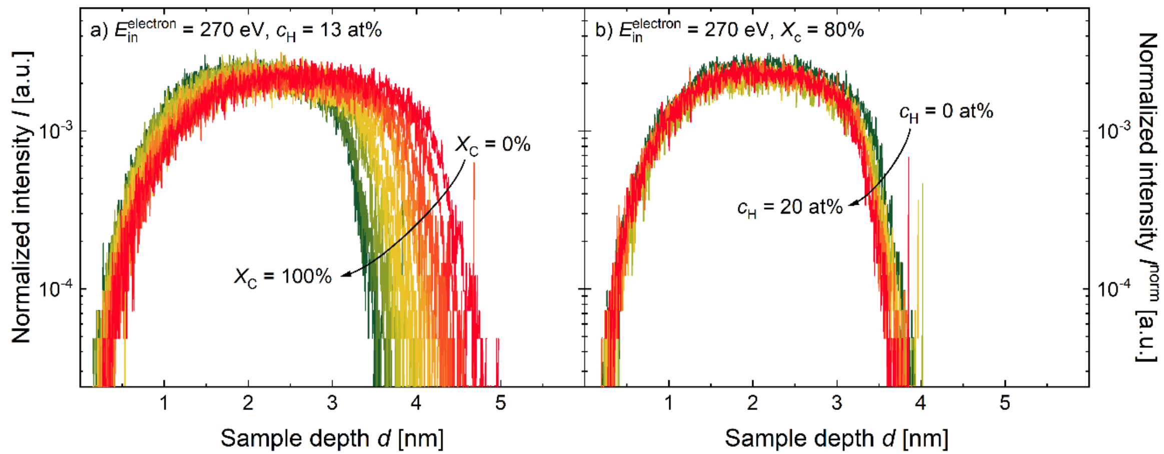

Figure S1. Penetration profiles of electrons depending on a) the crystallinity of the sample and b) the hydrogen content of the layer. While a lower crystallinity increases the penetration depth, no trend is visible for the hydrogen content.

Figure S2 shows the x-ray generation profile for varying incident energies of electrons. The simulated on-set for x-ray generation is 290 eV, and then only within the first 0.3 nm of the material. For higher energies of up to 500 eV, the x-ray generation depth increases to up to 9 nm.

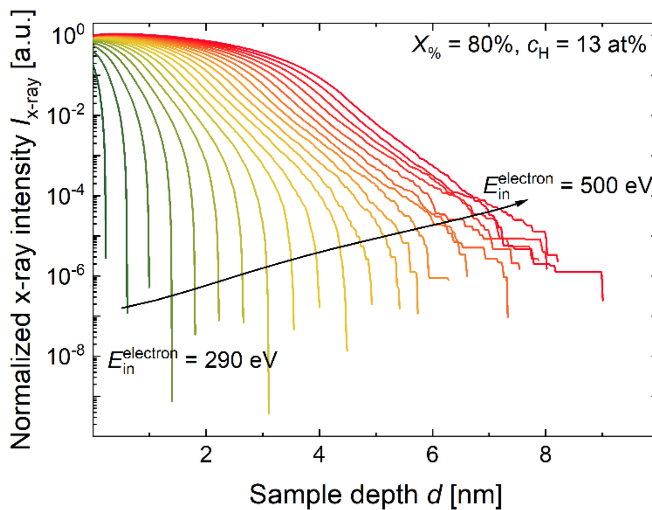

Figure S2. Simulated x-rax generation profiles for incident electrons with energies varying from the on-set of x-ray generation, 290 eV, to 500 eV. For the given real process parameters, no x-ray generation is expected.

S2. Additional Simulations for Ion Penetration

Addition simulations of the ion penetration depth regarding different material properties were carried out to further rule out different input uncertainties.

A variation in incident energy can be found in **Figure S3**, where in the incident energy of oxygen ions $E_{\mathrm{in}}^{\mathrm{oxygen}}$ is varied from 150 eV to 750 eV, which includes any doubly charged ions. For $E_{\mathrm{in}}^{\mathrm{oxygen}}$ of 150 eV, the penetration depth is only around 3 nm. For the single-charged ion at the given material properties the penetration depth is around 4.4 nm and for the double-charged oxygen ion, equalling incident energies of 550 eV, it is 7.8 nm. With the highest simulated incident energy of 750 eV the oxygen ion is penetrating 8.1 nm deep into the hydrogenated nanocrystalline silicon carbide (nc-SiC:H).

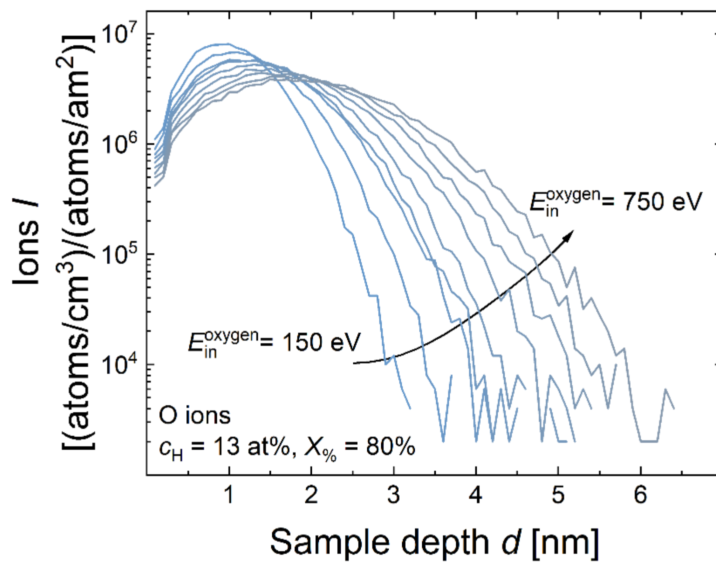

Figure S3. Simulated ion implantation depth for an oxygen ion at incident energies ranging from 150-750 eV. With the estimated material properties, even with the highest incident energy the penetration depth is far below 10 nm.

As for the simulation of the hydrogen content, it is assumed that the hydrogen content does not significantly change the density of the material, as it is supposed to be found on the corners of the crystallite and solved in the amorphous matrix. As can be seen from **Figure S4**, a variation in

the content c_H between 4.8 at% and 20 at% does not significantly change the penetration depth

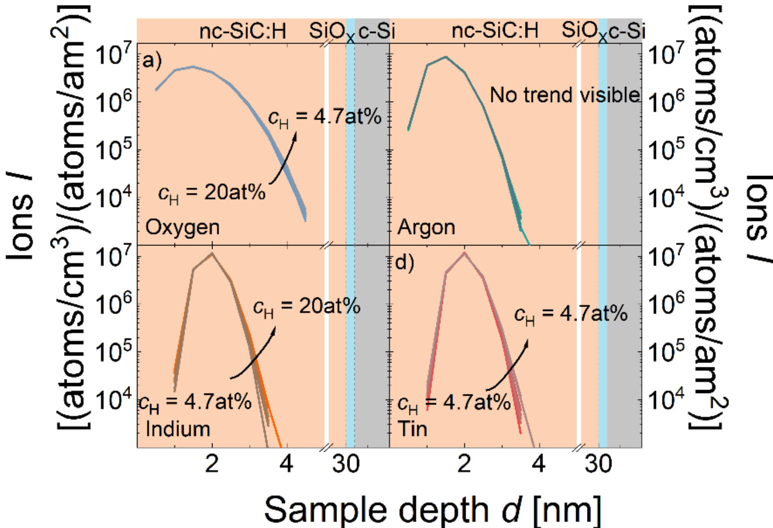

on any ion involved.

Figure S4. Influence of the hydrogen content on the penetration depth of a) oxygen, b) argon, c) indium and d) tin ions. No clear trend depending on the hydrogen content of the layers is visible.